Endcap Muon Alignment Project

June 23, 1999

1. Introduction

The *EMU Alignment Project* is organized around the need to locate (measure the actual position of) each of the 360 endcap cathode strip chambers (CSC) w.r.t. the Tracking System, with the required accuracy. It is part of the overall Muon Alignment effort, which also includes the *Barrel Muon Alignment* and the *Link System.*

The *Barrel Muon Alignment System* is built around a rigid and dimensionally stable latticework called MAB (Module for Alignment of Barrel). There are 6 MABs attached to the barrel yoke at each end of the barrel, 60 degrees apart in ϕ. Another 24 MABs are located in the spaces between the barrel wheels. Digital cameras are located at different points on the MABs, viewing point light sources on the barrel Muon stations. The MABs position are determined and related to the tracker coordinate system by the Link Alignment System. The EMU Alignment System will use 2-D sensors attached to the MABs, and will rely on the MABs position and rigidity to align the CSCs in ϕ, R and Z **[1]**.

The *Link Alignment System* will monitor the position of the central Tracker using laser sources and transparent 2-D sensors. Its function is to reference the Barrel and Endcap Muon systems to the Tracker coordinates. Each Link system ? plane is defined by measurement of three points in the tracker (via the Link laser and sensors) plus laser levels. This plane is then turned and projected onto two MAB sensors. With these point measurements, MAB laser levels and MAB calibration, the position of the MABs and our reference point sensors mounted on these MABs are defined in the Central Tracker system.

The Barrel Muon Alignment System and the Link Alignment System are the responsibility of the European Collaborators.

The *EMU Alignment Project* task is to determine and monitor the position of every CSC, to the required accuracy, relative to each other and to the MABs (and therefore to the central Tracker). It will be designed around three types of position sensors: a 2-Dimensional transparent position sensor, a wire extension potentiometer, and a proximity sensor. The last two types are off-the-shelf items and will be used for R and Z measurements, while the first one is being developed for use as straight line monitor (SLM) sensors. Additional information about the Muon Alignment System can be found in Ref **[1]**.

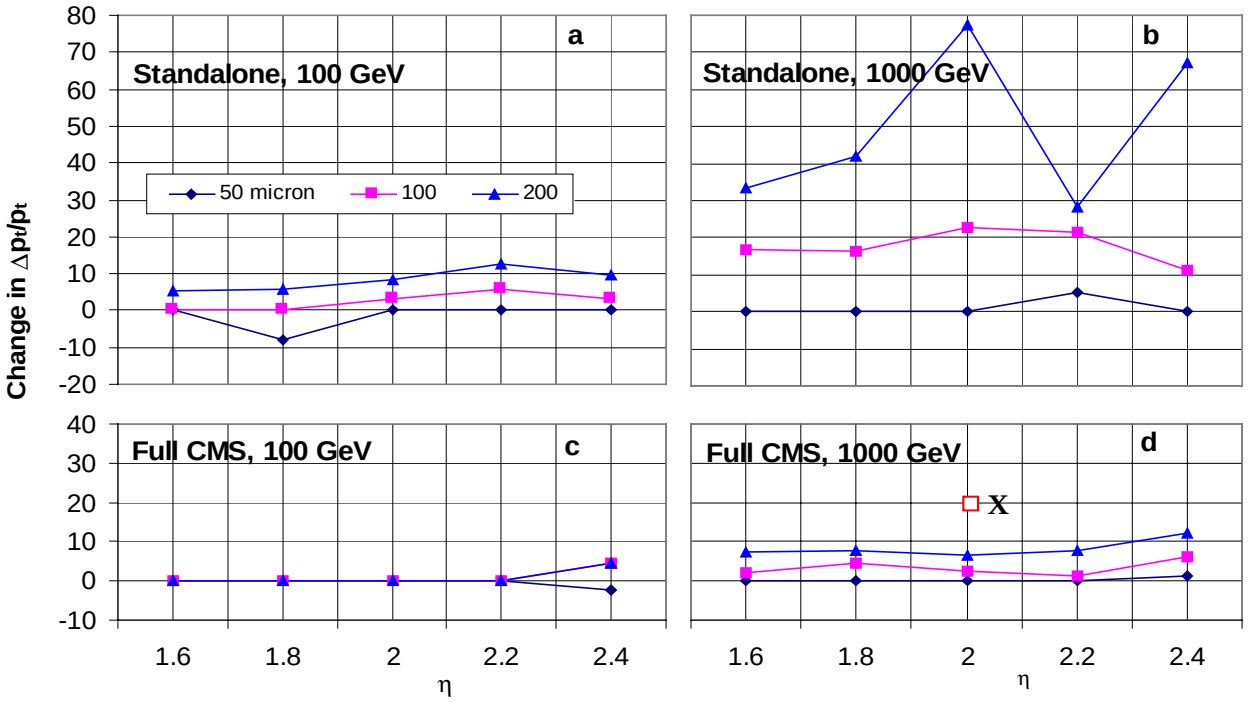

Fig 1. Percentage change in pt resolution due to alignment errors of 50 μm, 100 μm, and 200 μm, respectively. Data for p_t = 100 GeV and p_t =1000 GeV, from Karimaki & Wrochna. The data point marked **X** is from Arce et al.

2. Monte Carlo Studies

The results of at least two Monte Carlo studies of the EMU alignment requirement are available. The earlier one [V.Karimaki and G. Wrochna, TN/94-199], assumes a resolution of 100 μm per individual CSC layer (underestimating the actual chamber resolution), and concludes even a 200 μm error in the Rϕ alignment would worsen the Pt resolution by less than 10%, for 1 TeV muons. The plots in Fig.1 show clearly that the alignment resolution has a stronger effect for the standalone measurement (vertex constrained) than for the full CMS momentum measurement. The data in those plots were extracted from TN/94-199, Fig 3.

A recent study [Arce, Matorras, Rodrigo, and Vila, March 1, 1999] uses the current expected resolution for the CSCs (75 μm for ME1/2 and 150 μm for the other stations). It concludes that the error in alignment, which will cause a 20% degradation in the full CMS P resolution at η=2.0, can be as large as 500, 150, and 100 μm, for muons of 100, 500, and 1000 GeV respectively.

There are clear differences in the results from the two Monte Carlo studies. The early one shows, for instance, that for 1000 GeV muons, a 100 μm misalignment error will worsen the momentum resolution by less than 5% (**Fig. 1-d**), while the recent study claims that the effect would be four times as large. This can be partially explained by the difference in the CSCs resolution used as input. Karimaki and Wrochna used the same resolution for all stations (100 μm per single layer), while Arce et al. used the values (75 and 150 μm) given in the Muon TDR. However, the input difference can not possibly account for the different results. For instance, the relative effect of a misalignment

error should be larger when the chamber resolution is assumed smaller, while the difference between the two results goes in the opposite direction. It is clear that additional studies are needed to clarify the situation.

Nevertheless, the Monte Carlo results, as limited as they are, do not contradict the common sense approach indicating that the alignment uncertainty should be comparable to the chamber resolution. Thus we will set as requirement for the EMU Alignment to have uncertainties in the Rϕ direction, of 75 μm for the ME1/2 and 150 μm for the other stations.

We plan to initiate other Monte Carlo studies to examine this and other more specific alignment issues, such as the reliability of the error estimates and the possibility of correlation effects. Assuming bi-directional measurements by the 2D position sensors in the system, we will run a SIMULGEO system simulation (simulation and reconstruction program for optical-geometry systems, CMS Note 1998/079) for revised error estimates. Multiple coulomb scattering planar rms errors will be derived at each radial end of each CSC ring in each layer in a revised CSC geometry/layout for CMSIM to help understand resolution limits.

3. Conceptual Design.

The EMU Alignment System has two functions: 1) to reference the EMU Chambers to the position of the central Tracker, and 2) to measure and monitor the position of the CSCs to the required precision in ϕ, R, and Z. For the stations ME2 and ME3 these two functions are separate and well defined, as will be described below. But, for station ME1 they are not, and for that reason they will be described separately.

Ideally, the design of a system follows the definition of requirements and constraints. In practice, it is always an iterative process. Requirements and constraints are ultimately shaped by reality. For instance in the case of the alignment in the ϕ coordinate, the most critical one for the p measurement, we might start asking for a pair of position sensors at each chamber. However, forced by CMS geometry constraints and economics, the system ends up aligning about one fifth of all the chambers, and will rely on photogrammetry measurements, iron distortion modeling/measurements, overlapping CSCs, relative position sensors, and CSC geometrical accuracy to determine the position of the other chambers. This will, in turn, impose additional requirements on the construction of the CSCs. Therefore we have chosen to present first the design of the system so that the discussion on the requirements can be made more concrete.

3.1 System Overview

The EMU alignment consists of five types of sensor arrangements for the transferring and monitoring of each of the ϕ, R, and Z coordinates, which are:

- The EMU transfer line,
- The Z tube-sensors,
- The SLM (Straight Line Monitor) arrays
- The R sensors.
- The ME1 variation,

The ϕ coordinate alignment is handled by the Transfer and the SLM arrays. These are similar to each

other in their basic configuration: a laser beam defines a direction in space that is picked up by several transparent 2-D sensors that use it to reference their own positions. The transfer arrays, or lines, run parallel to the CMS Z-axis and along the outer cylindrical envelope of CMS, at six point separated by 60 degrees in ϕ. The SLMs run over the surface of each of the CSC stations, along radial directions, and join two diametrically opposed Transfer lines. Each SLM line starts near one of the Transfer lines and ends near another, and uses them as ϕ reference. The two Transfer lines and the SLMs that join them are almost on a plane called 'alignment plane'.

The Z tube-sensors are carbon tubes with proximity sensors a one end and position calibrated plates at the other. They transfer the Z coordinate to the SLM arrays.

The R sensors are string-potentiometers that will transfer the R coordinate from the Transfer line to the CSCs, along the SLM paths.

The ME1 variation is the ad-hoc solution to the alignment of the ME1/2 chambers. The ϕ coordinate for the CSCs is extracted in a manner similar to the SLMs except that the reference beam is now splitted off from the primary Link line (used by the Link Alignment System).

3.2 The EMU transfer Lines

The transferring of the Tracker's ϕ and R coordinates, to the EMU chambers, is achieved with the help of the outermost MABs. Bi-directional 2-D sensors will be mounted on the outer end of these MABs (both barrel ends, twelve sensors total) every 60 degrees around the periphery of CMS at R=7250mm. Six laser beams will be projected from the far end of each Endcap and their orientation measured by these 2-D sensors on the MABs. The 2-D sensors are accurately positioned on base plates, called Transfer plates, which are attached to the EMU Stations. The laser beams and sensors define the EMU transfer lines, and determine the R and the ϕ reference coordinates for the Endcap stations**.** Two laser beams coming from opposite directions thus define each EMU transfer line, which gives it a high degree of redundancy. Two diametrically opposite EMU transfer lines would in principle define an R-ϕ plane that contains the LHC beam line. In reality, due to the mirror symmetry of the barrel muon system, and to the beam pipe, the EMU transfer lines are not truly diametrically opposite. The plane defined by these lines, and shown in **Fig. 2**, does not contain the CMS axis.

Two possible optical beam position sensors are under development/test for these transfer lines; ALMY [**2,3 ,4**] and our DCOPS [**5,6,7**].

Each EMU transfer line is implemented with:

- 2 laser sources, one at farthest iron plate of each Endcap ➔ 12 laser sources
- 8 2-D sensors, 1 per station and 2 on the MABs. ➔ 48 2-D sensors
- 6 base plates (transfer plate) to support the 2-D sensors. ➔ 36 transfer plates

In addition a certain number of spares (5%-10%) are needed. This also applies to all the other component lists that follow.

Note on naming convention: Previous descriptions of the Alignment system have used the name 'EMU link line', now obsolete, instead of the present 'EMU transfer line'. We decided on this change after we found that the word 'link' was also identified with the Link Alignment System and its use in the EMU Alignment was very confusing. However, earlier references and drawings still contain the obsolete name.

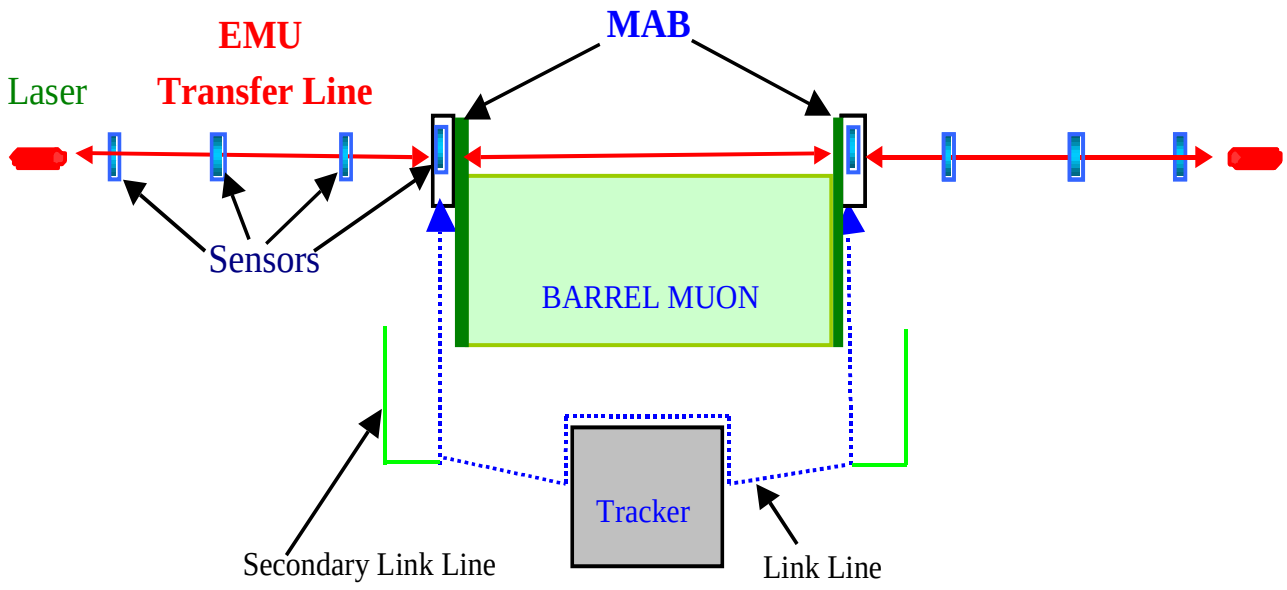

Fig 2. EMU Transfer-line Schematics

3.3 The Z Referencing.

The Z coordinate for each EMU station will be transferred from the MAB to the transfer plates, at six points around the station as shown in **Fig.3**. This will be done with carbon tubes instrumented with proximity sensor at the end furthest from the transfer plate. Proximity sensors of two different ranges will be required: one with a range of several centimeters, near the MAB, and the other with a range of few millimeters, between the stations. The difference is important, since the price of the long-range sensor is about 40 times higher than that of the short range one.

Z components of EMU transfer line:

- 2 carbon tubes with long range proximity sensor ➔ 12 carbon tubes and LR proximity sensors.
- 4 carbon tubes with short range proximity sensor ➔ 24 carbon tubes and SR proximity sensors.

3.4 The CSC SLM Arrays

At six points on the periphery of each Endcap station there will be a laser and a reference point sensor, attached to the Transfer plate, which will carry the ϕ, Z information across the surface of the CSCs. Two 2-D sensors on each CSC along that laser direction will give the ϕ orientation of those chambers. We call this arrangement of lasers and 2-D sensors a SLM array, or line.

We have developed a solution to the configuration of these Straight Line Monitors and Transfer lines, and plates, that provides a uniform and mirror symmetric crossing across the CSCs. This minimizes the number of sensor positions (holes and pins) on the CSCs and allows for universal substitution in position and for standardized mounts and parts (see **Fig 2a**).

The chambers not provided with 2-D sensors will be aligned in ϕ through their overlap with their

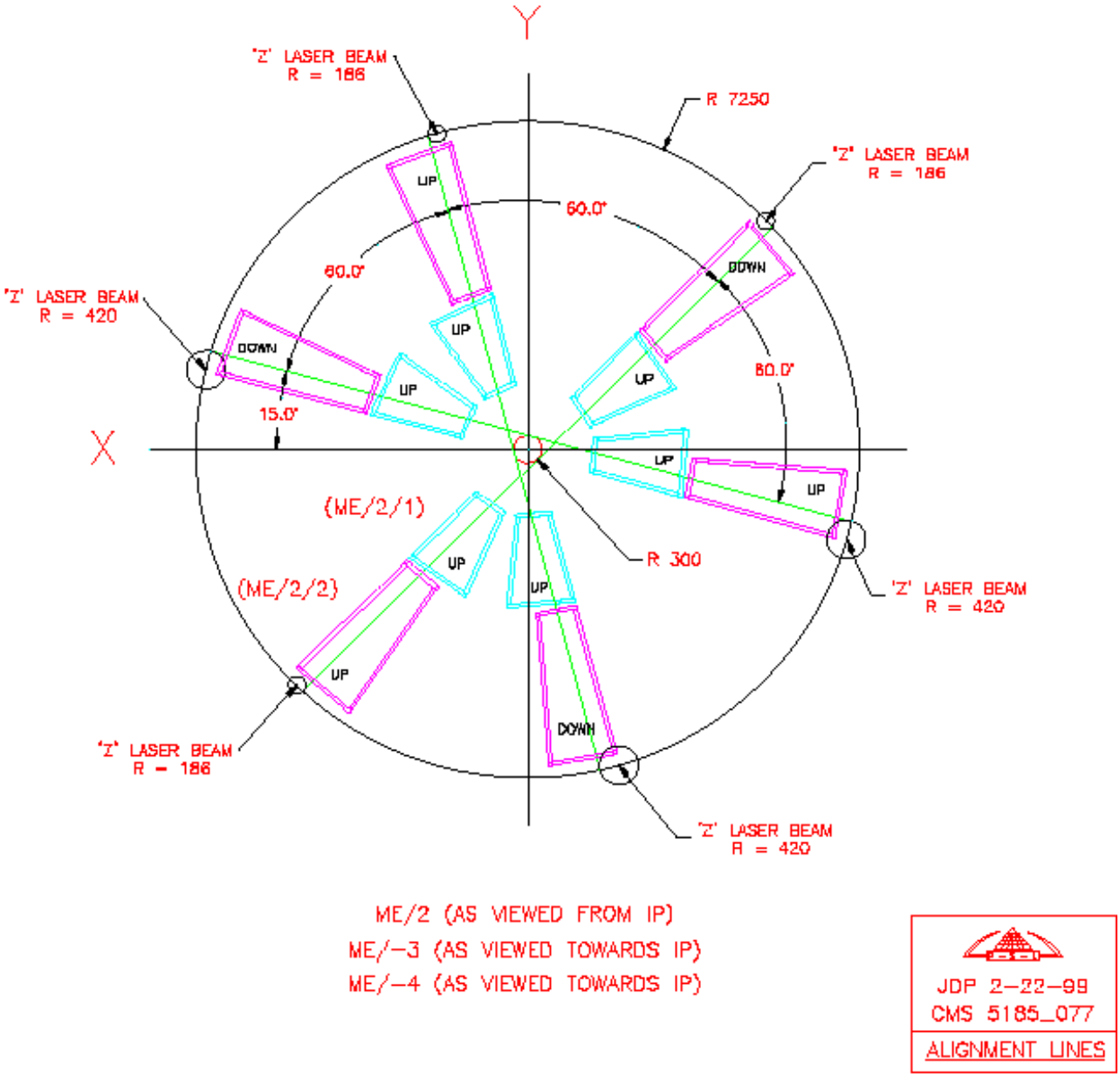

Fig 2a Definitions of the SLMs orientation on station ME/2. Only the CSCs that will be fitted with 2-D sensors are shown. The six small circles around the R 7250 perimeter contain the interception of the EMU Transfer lines (at its centers), and the location of the SLM lasers (at the points of tangency). Notice that the circles are of two different radii; that was needed to accommodate the quasi 60 degree symmetry of the SLMs to the mirror symmetry of the Transfer lines.

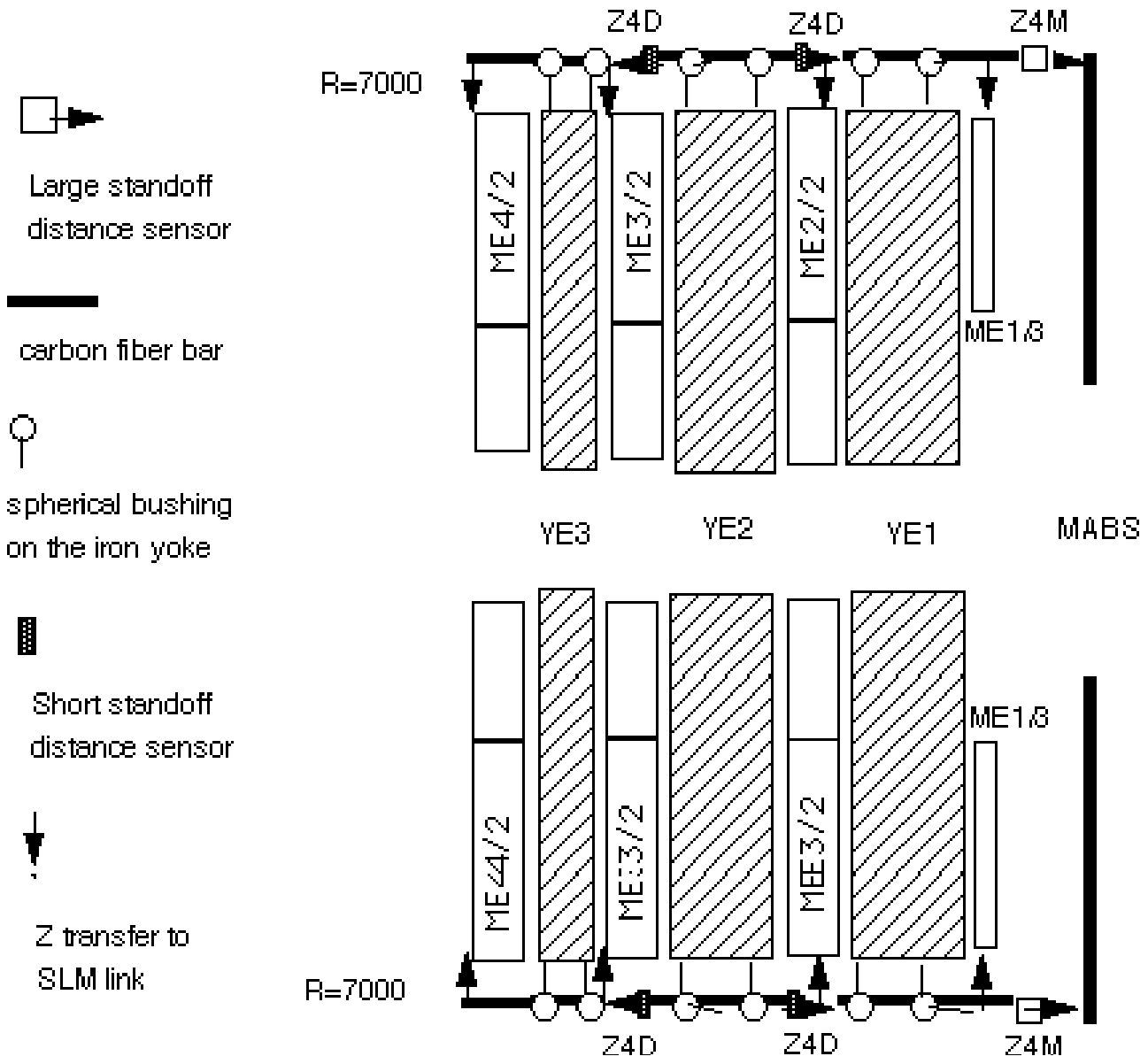

Fig 3. Schematics of Z-alignment (ME4 has been de-scoped out, but still remains in earlier drawings like this one).

neighbors. As will be discussed below, this procedure will rely on a precise knowledge of the R position of the strips, as well as in the precise machining and referencing of the strips themselves.

The same laser (the SLM laser) that carries the ϕ information will also carry the Z coordinate to the CSCs. Only the chambers under the SLM lines will have their Z position monitored. The Z behavior of the other chambers will be interpolated from the measured chambers and model deflections for the

iron.

Components, per SLM:

- 2 lasers, one at each EMU transfer line at opposite ends of the SLM line ➔ 36 laser sources
- 10 2-D sensors, one attached to each of the laser sources, and 2 on each of the 4 CSCs under the SLM line, ME1/2 Endpoint ➔ 192 2-D sensors
- 8 (10) SLM sensor brackets to locate the 2-D sensors on CSCs ➔ 150 SLM plates of 6 types (ME2, ME3), 6 types (ME1) plus spare sensors and lasers (5%).

3.4 The CSC R Position Monitoring

The R coordinate on an outer chamber under the SLM line is determined with respect to the EMU transfer line. A linear potentiometer will measure the R distance between that outer chamber and the transfer plate (that contains the EMU transfer sensor, the SLM laser, and endpoint reference sensor). Another potentiometer of the same type will monitor the R-distance between the outer chamber and the inner one. The scheme relays on the precise knowledge and stability of the CSC's physical dimensions.

The R position of the chambers not under the SLM lines may be measured against the neighboring chamber, using a linear potentiometer of the same type as above. We can calibrate these using the detailed photogrammetry of each open layer after assembly knowing their readout values and derivative. We do not have to make precision internal transferring.

Charged particle tracks may be used to determine, and even monitor, the R position of the chambers. The boundary between wire groups could be located with adequate accuracy, using information from the tracking system. Simulation studies will be undertaken to have a better idea of the measurement uncertainty under realistic conditions.

Components:

- Up to 1 linear potentiometer per chamber ➔ 360 potentiometers
- Brackets to support/connect the potentiometers ➔ 720 brackets.

3.5 The ME1 Variation.

The ME1 station is the only one that has three rings of CSCs. The innermost ring, the ME1/1 station, is the responsibility of JINR Dubna, and its alignment will be designed and instrumented by our European colleagues, hence it will not be mentioned in this work plan.

The alignment design for ME1/2 is different from that of the other stations. Here, because of geometrical constraints, and of the proximity to the primary Link lines, the ϕ information will be obtained from laser lines parallel to the primary Link lines. Those 'secondary' laser lines, supplied by the Link Alignment Group, will be generated by splitting each of the six primary Link lines with a rhomboid prism. The Link Alignment Group is still optimizing the physical location of those prisms, on the endcap iron. The necessary components are the same as for the SLMs except possibly for the laser sources, and are included in the components list. Another important benefit from the ME1 variation is that the alignment error is smaller than for the other stations because the coordinate referencing error is substantially reduced.

The secondary Link lines will only align 6 chambers out of the 36 in ME1/2, just as in the case of the

SLMs. The bulk of these chambers will be relatively aligned in ϕ by photogrammetry, and will be monitored??using particle tracks through the overlapping sectors of the chambers.

The R position will be derived from the R tubes used by the Link system to transfer R to the MABs. We can make relative radial-position measurements between all pairs of the ME1/2 CSCs. Their radial-positions will be measured in photogrammetry of this layer.

Because it is not possible to see across the whole ME1 layer (due to obstruction by spacer blocks and other geometry constrains), the ME1/3 Straight Line Monitors are established by six outer Endcap Transfer-line points (laser sources and outer reference endpoint sensors) and six inner endpoint reference sensors mounted on the ME1/2 CSCs that are measured-monitored by the secondary link-lines. These inner reference points are better (smaller errors) than an opposing Transfer point. Again we can make relative radial position measurements as well as six absolute R links to the Transfer plates and six to the ME1/2 located by the Link R transfer tubes. The outer non overlapping ME1/3 CSC layer also requires Rϕ proximity sensor measurement at each end of one radial edge of these CSCs to provide a ϕ measurement for all of the CSCs. The non-radial ME1/3 SLMs path must clear the Z stops between the Barrel and Endcap iron rings.

3.5 Components Summary

Table 1 shows a list of all the elements to be used in the EMU Alignment system. Cables, computers, power supplies, and other such auxiliary items are not included.

Table 1. Components Summary

Component Name	No. Per line/position	Total components	Total lasers	Total 2-D sensors	Total Plates
Transfer Lines					
Laser sources (one at farthest iron plate of each Endcap)	2	12	12		
2-D sensors (1 per station and 2 on the MABs)	8	48		48	
Transfer plates to support the 2-D sensors.	6	36			36
Z-sensors					
Carbon tubes with long range proximity sensor	2	12			
Carbon tubes with short range proximity sensor	4	24			
SLM Lines					
Lasers, one at each end of the SLM line	2	36	36		
2-D sensors	10	192		192	
SLM sensor brackets or plates	8	150			150
R Sensors					
Linear potentiometer	1	360			
Brackets to support the potentiometers	1	720			720
Temperature Sensors					
T-sensors	1	468			
SUM		2058	48	240	906
Spares		116	4	24	10
Total Components		**2174**	**52**	**264**	**916**

4. Precision Requirements.

The precision requirement on the EMU alignment system is determined by two different, though related needs. The first one is for triggering. The better the ϕ coordinate measurement is, at the trigger level, the better the low momentum background rejection will be, and the more efficient the experiment becomes. However, at the trigger level, the ϕ measurement granularity, per pair of layers (6 layers per CSC), corresponds to one half of the strip width (12mm average). This means that the alignment Rϕ resolution need only be about one to two millimeters to avoid degrading the trigger uncertainty.

The second need for a precision measurement of ϕ is to measure the bending angle of the muon of interest, to determine its momentum with the best possible accuracy. The momentum measuring capability of the EMU system sets the requirements for the position resolution of the Alignment System. The momentum measurement is limited by the transverse (Rϕ) resolution of the CSCs and multiple Coulomb scattering. Thus, the EMU alignment should at least match the resolution of the CSCs.

Arguments for looser constraints in the Alignment system are based on the possibility of using actual tracks to refine the alignment of the chambers. It unclear that this is a practical option for short-scale real time effects. For one thing, the multiple scattering in the material before and between the EMU stations will limit the usefulness of the low momentum muons, which are the most abundant. Then, the residual magnetic field in the iron will not be easily modeled to the required precision. The time and effort involved in the procedure will, even in the best of cases, limit its frequency and timeliness. On the other hand, a looser constraint on the alignment, perhaps a factor of two or five, will have almost no impact in the cost and effort involved. As will be detailed later, most of the cost of the alignment system comes from the readout electronics and mechanical attachment of about one thousand rather inexpensive sensors. However, the precision requirement will dictate the required level of CSC assembly control and measurement, sensor calibration, correction, and stability. There are many complicating factors including the thermal and gravity behavior of the CSCs that must be understood on the corresponding level. Also the stability of the cathode machining coordinate system, external fiducialization accuracy, and 3D rotational positions of the CSCs, etc, become very important factors limiting the achievable in situ precision. We intend to implement every CSC with photogrammetry target brackets (at the sensor pin locations) that allow magnet-off planar measurement of the CSCs. With ϕ symmetry in the iron and support, only small field-on tilting of the CSCs in Z on their kinematic mounts should occur.

TABLE 2

Alignment Precision Requirements (in μm)			
Station	**Rϕ**	**R**	**Z**
ME1	75	430	~1000
ME2,3/1	150	430	~1000
ME2,3/2	150	860	~1000

The Monte Carlo results, presented earlier, indicate that the required alignment resolution can be much larger than the CSC resolution, at momenta below 100 GeV. However, at higher momenta, where the muon chambers are most important, the alignment resolution should be at least comparable to the CSCs resolution. **Table 2** summarizes these considerations. Regarding the precision requirements on R and Z, both Monte Carlo agree that the momentum measurement, even at high momentum values (Pt ~ 1 TeV), is insensitive to alignment errors of order1 mm. However, as described later, we have calculated that for radial strip patterns there is a direct coupling between R alignment and Rϕ accuracy. The constraint in Rϕ will then translate into an R alignment constraint stricter than that coming from the CSC R measurement resolution. The latter is determined by the wire-group width, which is 16-19mm for the inner CSCs and 51mm for the outer ones.

4.1 ϕ Alignment Requirements.

The expected alignment error in the position of the CSC assembly (in real time) is required to be smaller than the chamber resolution, in order not to degrade the overall momentum measurement.

The Rϕ resolution requirement for the CSCs is determined by the multiple scattering on the muon tracks within the momentum range of interest (Pt<100 GeV). Thus specific spatial resolution requirements for the CSCs were set, after detailed Monte Carlo studies of the CSC characteristics [Muon TDR, 4.1.2.2], for the ME1/2 chambers (75 μm) and for the other Endcap chambers (150 μm). Therefore, the alignment system should be able to tell the ϕ location of each chamber to better than 75 μm (in Rϕ), for the ME1/2s, and to better than 150 μm for the other CSCs [Muon TDR, 7.1].

4.2 R Requirement.

The CSCs limit the R position of a track through signals coming from groups of HV wires. Those wires are ganged into groups of between 5 and 16 wires each, depending on the chamber location within the EMU system. Thus, the granularity of the CSC R measurement is limited to 16-19 mm for the inner ring CSCs [Muon TDR, Table 4.1.1], and to 51mm (35mm) for ME23/2 (ME1/2). However, the required precision in the R-position measurement, is dictated by the ϕ alignment requirements, and is a factor of 20 to 50 more stringent than the R limit from the CSCs. This means that the relative and absolute R-position of the chambers must be established, and ultimately located by survey and the Alignment System. The relative R-position of the chambers will be established by the accuracy of the CSC mounting holes on the Endcap steel plates (and will be checked by Kawasaki half ring and CERN whole ring photogrammetry). Absolute R will be measured across the CSCs along the straight-line monitor paths in relation to the CMS R coordinate given by the transfer-plates and transfer-lines. We will have to understand the dimensional behavior of the CSC upper panel (vs. temperature) by tests as we use the CSC panels as rulers. These twelve radial measurements will provide redundancy in locating the CSC layer ensemble in the CMS coordinate system. However, this system does not find any intermediate-unmeasured “rogue” CSC that may have “fallen out of place”. Only relative R measurement between CSCs (or a many track analysis of overlap strip tracks) can provide relative R information at any point in time after the original survey. Then in a consistency fit of the string of CSCs between SLM lines, we can check radial positions.

4.3 R-Positioning of the CSCs.

The measurement of a track R-coordinate is limited by uncertainties of up to 15 mm, without affecting much the ϕ measurement. However, a relatively small misalignment in the R position of the chamber

can cause a noticeable error in ϕ. This can be seen in **Fig. 4,** where a set of radial strips, 20 degrees wide, is shown displaced from its intended position by a radial distance ΔR. If one assumes that the left strips are properly aligned in ϕ then, because of the radial displacement of the chamber, the ϕ reading would be shifted by ever increasing amounts as one moves away from the reference edge. The effect is clearly larger for the 20-degree chambers than for the 10-degree ones. The partial error in R translate into an Rϕ contribution given by the simple formula

$\Delta(R*\Phi) \approx \Phi * \Delta R$

where Φ is a fixed angular interval.

For the 20-degree chambers, the Rϕ error, at the farthest strip, would be 350 μm for each millimeter error in R! It will be half as bad for the 10-degree chambers. Notice that the error in ϕ does not depend on the absolute R-value; thus the ϕ error worsens as the radial distance becomes smaller.

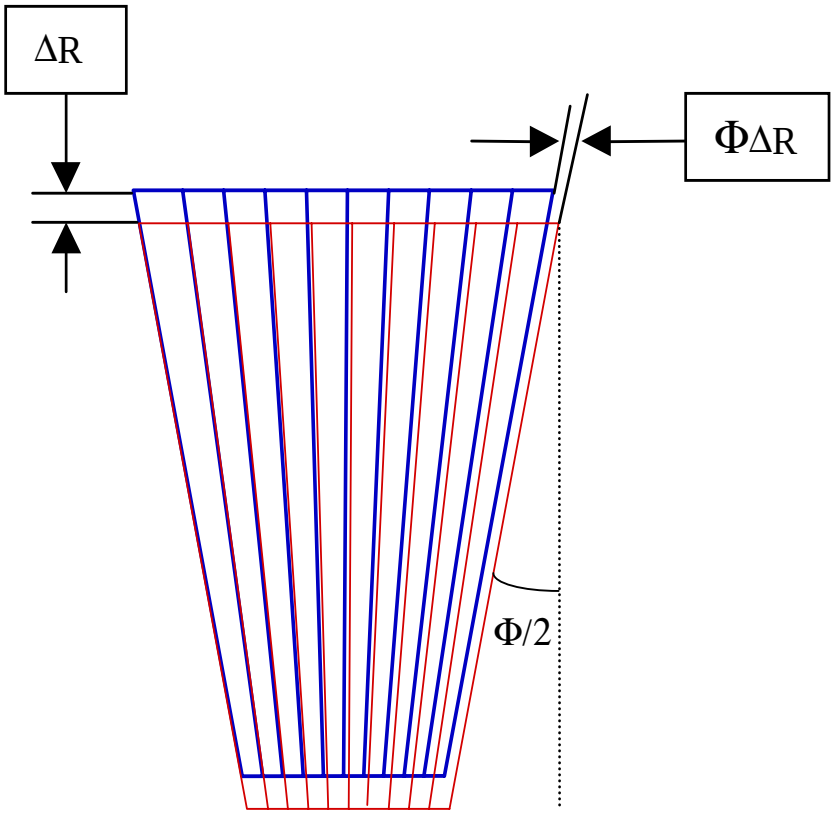

Fig 4. Strip R Displacement effect.

As was mentioned earlier, the EMU Alignment will use the chambers as calibrated ϕ intervals in order to measure the strip positions away from the CSCs that are under the SLM lines. The accuracy of those ϕ intervals depends on the R-position, then given the requirements for the Rϕ error to be under 150 μm, we can state the requirements for the R position of the chambers. The actual R position of the strips should be known to better than 430 μm for the 20-degree chambers, and to better than 860 μm for the 10-degree chambers. The constraints are tighter, by a factor of two, for the ME1/2s, namely the R position of the strips should be known to better than 430 μm, even though the chambers there are all 10-degree. In the ME1/2 and ME1/3 rings we monitor the relative ϕ positions of both ends of the intermediate CSCs given panel dimension constraints, we can solve for the best fit of these CSC ϕ positions.

If we were to estimate the Rϕ error starting from the center strip, the effect of a 1 mm change in R would be half as large (175 and 88 μm, for the 20 and 10-degree chambers respectively). But that would understate the error in transferring the ϕ information from one CSC to the neighboring one.

The reason for this sensitivity on R is that the CSCs have been designed to directly measure the ϕ coordinate of a hit. By construction, the spacing between strips is proportional to their distance to the CMS Z-axis, namely to absolute R. In other words, the strip spacing carries the design value of R at every point of the strips, and when the actual R-position does not match the design value, the strip spacing is no longer a good measure of ϕ. It is interesting to note that although the measurement of ϕ is so sensitive to the absolute R distance, it is not so much the R-value of the individual track that matters, but the R position of the radial strip pattern.

Since ϕ is so sensitive to R, could we deduce the R position of a chamber by using the ϕ information from overlapping strips? The answer is yes, but only if we know the ϕ location of overlapping strips at both sides of the chambers.

The twist or rotation of CSCs on the face of the distorted iron should be small because of the magnetic ϕ symmetry. The major change should be a tilt in Z. The slope dz/dr is approximately constant. The effect on the projected CSC strip definition should be small.

4.4 Z-Requirement

The requirements on the Z-measurement are looser than for the other coordinates. The Z-position is important for the tracking on the R-Z plane, the non-bending plane, where anything similar to the current CSC R-resolution would be sufficient. The effect of a Z misalignment on the ϕ measurement, either directly (rotation around R) or through an R shortening (rotation around one of the short sides of a CSC), are very small. At worst, it is a '1-cos' effect. A 1-cm error in Z will have a negligible effect on ϕ.

The total expected Z deviations, due the deformation caused by the strong magnetic field, are at worst 1-2 cm. The alignment sensors need to be able to accommodate that dynamic range. This is marginal for both of our sensor/laser options. Inner sensors on the MEn/1 rings will have to be set low (field off). In addition, the laser beams from each transfer-plate end will have to be displaced, rotated between field-off and field-on conditions in order to get across the layer and through the sensors.

More realistic estimates may put the Z deflection beyond present sensor range. That will force us to

modify the sensor design to accommodate a doubling of the sensitive range in the Z direction.

The Z-position of the CSCs will be measured and monitored for only the chambers under the alignment lines (20% of the total) to better than 0.5 mm. The Z-position of the non-monitored chambers will be estimated, to within a few millimeters using the ANSYS distortion model of the iron discs. Hopefully iron distortion measurements in magnet tests will calibrate this model.

5. Detailed Design

5.1 The EMU Transfer and the Station Alignment

Both of these subsystems use the same basic technique: a laser source defining a direction in space, and transparent 2-D sensors that will measure the position of the laser beam at various points along its path.

The specific sensor type, as well as the type of laser to be used, has not been decided yet. This issue will be discussed in more detail in a later section. The two sensors under consideration are similar enough, in their operation, that only minor details of the design, at the present stage, would be affected by the choice. We are designing a standard mount consistent with both.

The baseline choice is based on transparent ALMY sensors, which require small beam spot, small-divergence commercial laser-diode sources. The alternative is to use COPS (CCD Optical Position Sensor) and lasers with cross-hair generators. These two sensors, as well as the results of the tests they were subjected to, have been described in some detail elsewhere. A brief description follows.

The ALMY I sensors have a 64 x 64 grid (X, Y) of 300 micrometer wide (312 micro pitch) photocurrent readout strip channels over a 20mm X 20mm active area of a 1 micrometer thick amorphous Si photo-diode (Shottky) detector sensing a laser optical beam. The sensor on a glass substrate is mounted on an aluminium support plate and embedded with a group of three interlocked circuit boards containing all necessary control and readout electronics. The readout features analogue multiplexing of all X or Y channels through a single input amplifier, so each axis is self-normalised. Each sensor includes an onboard ADC and RAM for the 128 digitised strip readings. The onboard electronics are designed to require no calibration. The sensor outputs are daisy chained into a standard VME crate through a custom interface. The ALMY memory and control functions are accessed with a standard VME system interface via a shared UNIX workstation. Failure of a sensor results in its address and data disappearance on the daisy chain.

The ALMY II sensors are to be an improvement on ALMY I eliminating internal reflection interference effects from the non flat (wedge) glass substrate via anti reflective coatings. They also feature more compact ASIC electronics. By increasing front-end electronic gain, the required laser power for a good signal has been greatly reduced, so ageing effects have been significantly reduced. With new anti reflective coatings the transparency of the detector at 780 nm has been increased to 80-90% making long strings (ten) of detectors with reasonable signal possible (reported MPA test results at CMS week, 15 march, 99).

We have experimentally studied the ALMY I sensor and have demonstrated adequate resolution in a half layer SLM test-bench [**8,9,10**]. We have also studied a Transfer line test-bench with ALMY I and

again demonstrated adequate resolution [**11**]. These sensors are under continued development at Max Planck Institute for ATLAS [**4**].

The light source is a commercial COHERENT or Melles Griot fixed optics laser-diode module.

The alternate SLM sensor, COPS, consists of four linear CCD arrays arranged around a square hole on a printed circuit board [**5-7**]. Each CCD contains 2048 pixels, with 14 μm pitch. A cross-hair laser defines a direction in space and its position is detected by the CCDs with intrinsic accuracy better than a micron. Since just two CCDs are needed to define the center of the laser beam, the other two CCDs can provide a high degree of redundancy, and can also measure axial rotations. The square hole allows the center of the cross hair laser to continue undisturbed and to illuminate all the COPS along the beam path.

The CCDs are inexpensive (~$14 each in small quantities) and commercially available. The laser source is a simple diode laser (~5 mwatt) with crosshair generator optics. Sharper crosshair lines, more suitable for large laser-sensor distances (over 10 m), can be obtained with two lasers and two cylindrical lenses.

The readout with a new digital board, which uses an on-board signal processor (DSP), will simplify greatly the data analysis. The output from the DSP's will give directly the laser beam position, as seen by the four CCDs. Several COPS can be daisy-chained in a serial network and controlled by a PC.

The digital COPS prototypes are being produced at Fermilab and will be tested at Northeastern. Improved versions of COPS are also under development, including the addition of bi-directional capability to the original design. Radiation hardness tests are to be started shortly.

5.2 Support plates and physical attachment

Sensors and light sources will attach to base plates, to be located with millimeter precision at appropriate places. The plates have two very crucial roles in the alignment system: they either transfer the Tracker reference coordinates onto the surface of the CSC stations, or reference the position of the sensing strips in the chambers to the actual sensor position. The EMU transfer-plates serve the first role, and the SLM plates, together with the R and Z-plates (whenever they are necessary), cover the second.

5.2.1 Transfer-plates.

The transfer-plates are the connection-coordinate linking plates for the active elements defining the EMU transfer and SLM lines. Each plate carries a 2-D sensor that picks up the position of the EMU transfer laser beam across CMS. In addition it carries another 2-D sensor and a laser source, mounted perpendicular to the EMU transfer line (**Fig 5**). That laser points towards the corresponding 2-D sensor on the diagonally opposite transfer plate, thus defining the SLM path across the CSCs surface. The rigid plate structure includes a two angle (θ, ϕ) precision inclinometer and a reference connection and transfer of the R, Z coordinates. After assembly this transfer plate with sensors will be CMM measured to establish the offset coordinate transfers between the Transfer-line and the SLM lines; that is we will measure the position relationship of the optical sensors. We will also check the calibration of the inclinometers. There are four different offset versions, and an equal number of mirror configurations, in different transfer lines and CSC stations.

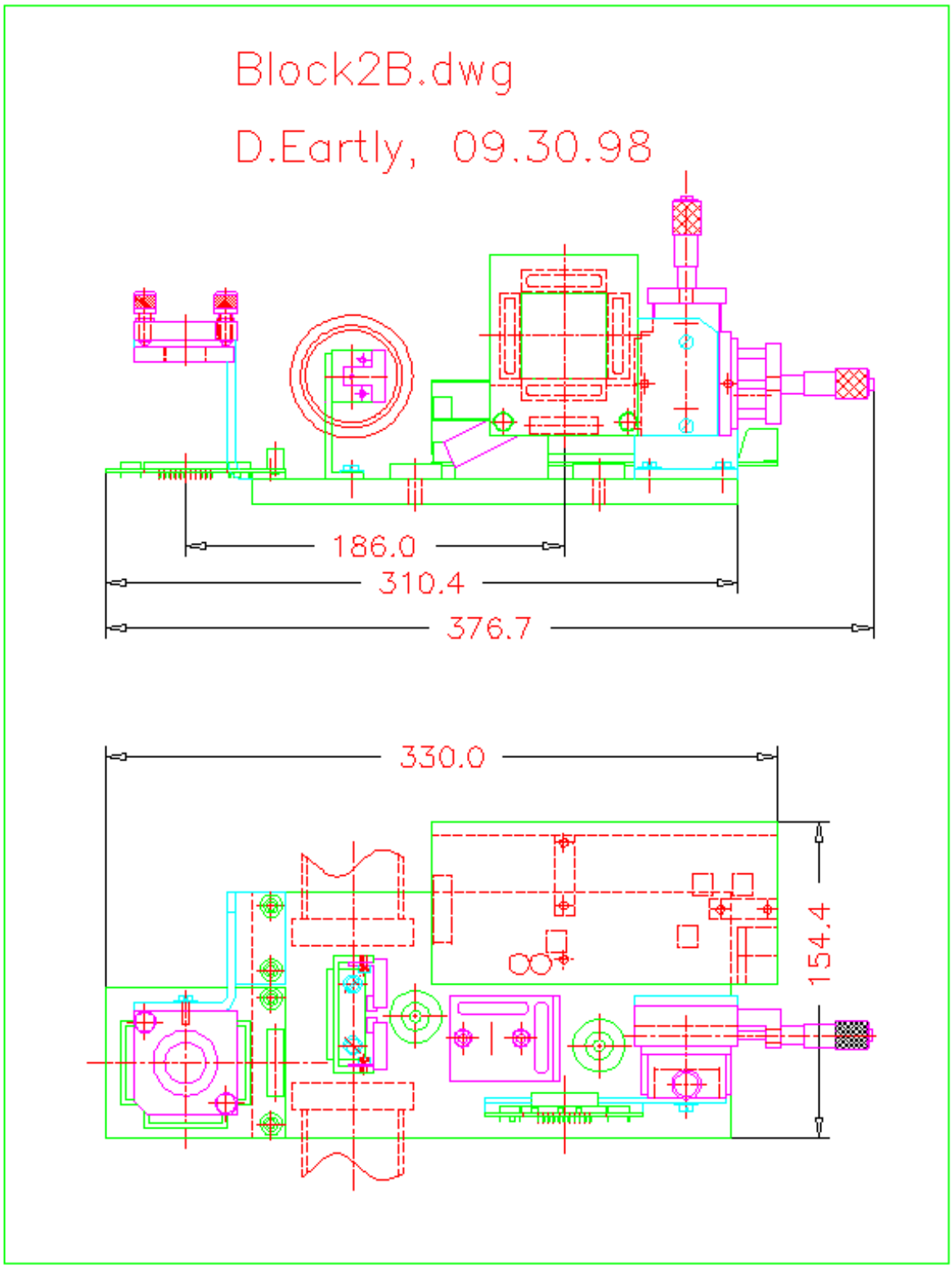

Fig. 5 Draft layout of a transfer- plate for the DCOPS sensor.

5.2.2 The CSC SLM, R Sensor Bracket.

Two 2-D sensors will be attached to the CSCs in the SLM path, on separate standard SLM sensor brackets one at each radial end. These brackets will be mechanically pinned-attached to mounting plates. The inner radius plate is glued directly to the top CSC panel. It is precisely referenced to the strips via a transfer fixture using two pins in the top CSC panel along the CSC small end gap bar bolt line. These holes in the top panel can be measured relative to strip end fiducials and the alignment pin to about 25 micron with special measurement tooling that has been built. On the outer radius large CSC end, the mounting plate sits on shoulder pins which rest on the frame but their position is referenced to the strip coordinates through the pins (holes) in the top panel surface along the gap bar bolt line. Again these can be measured relative to the strip end fiducials with good precision. Shims and variable pin shoulder lengths allow for Z adjustment of alignment sensor position to compensate for magnetic field motion and to maximize sensor dynamic range. The R transfer sensors are also on these mounting plates and will be calibrated. The plates and brackets will include calibrated retro-reflective strip targets for digital photogrammetry

5.2.3 The R and Z-sensor plate

The Z sensors will be attached to the Endcap Transfer plates, and the R-sensors to the SLM sensor plates. These sensor locations will be established by CNC machine tolerances on mounting brackets and holes. R sensors (potentiometer extension can be calibrated relative to the pins in the SLM mounts which reference the top CSC panel and strips. Z sensor positions (front faces of Z4W sensors will be measured in the CMM of the Transfer plate assemblies. Proximity sensors between CSCs will be mounted on their own brackets, and attached to a CSC frame, and have their initial location measurement done with digital photogrammetry and mechanical gauge measurement. Displacement calibration will be done with the standard bracket in a laboratory calibration fixture.

6. Implementation

6.1 Calibration

The different sensors must be positioned on their support plates or brackets within specified tolerances. Displacement calibration tables must be created in order for the alignment system to satisfy the design accuracy. The following paragraphs will list the necessary calibration goals, while the next section, describing the initial alignment procedures, will make it clear why those constraints are needed.

The 2-D sensor position will be calibrated with respect to fiducial marks on its support plate (transfer and SLM). The accuracy in its position will be better than 25 μm in the Rϕ direction, and better than 0.2 mm in the other coordinates. Its orientation will be calibrated to within several mrad. The same precision is required for the 2-D sensors on the MABs, which will define the coordinates of the EMU transfer-lines. Adequate photogrammetry targets will be included and measured on CSC sensor brackets, transfer-plate, and MAB sensor mounting assemblies. All of this can be done at a calibration station.

The EMU transfer laser mounts and adjustment on the ME3 transfer-plates will be measured with respect to the transfer plate fiducial marks (to which the SLM laser and 2-D SLM endpoint sensor

are also referenced). However, these lasers will have to be adjusted in angle and position during CMS assembly (Endcap-Barrel closure) to thread the laser beam through the MAB sensors (20m beam path-length) with adequate dynamic range available.

The Transfer-plate assembly includes R and Rϕ adjustments on the transfer-line 2-D sensors, which will allow all sensors in the 20m laser-line path across CMS to be positioned with adequate dynamic range. This micrometer adjustment must be pre calibrated to maintain the coordinate transfer accuracy between the Transfer sensor, transfer-plate, and SLM endpoint sensor.

The Transfer-plates will include precision (θ, ϕ) inclinometers which will be checked and measured in calibration. The Transfer-plates will include precision (θ, ϕ) inclinometers (0.1745mrad resolution) which will be checked and measured in calibration. With the CMM measurement of the transfer plate assembly, they define the transfer plane between the transfer and the SLM endpoint (definition) sensors. The R error for different transfer plates varies from 32 to 73 microns, but the Rϕ error is negligible. The Z position transfer error is determined by mounting of the transfer plate support structure to the corner plates of the iron discs and the location tolerances of the corner plates. We give a preliminary estimate of 100 microns for the Z transfer error. Otherwise the error is dictated by digital photogrammetry.

Z, R, and Rϕ proximity sensors will be calibrated in a standard automated test-bench with computer logging. Offset, slope, and range will be measured. The calibration of a sensor will take a few minutes and the results will be databased for software reconstruction. M1/3 proximity sensors will be mounted on extensions of the SLM outer/inner sensor brackets. While the ME1/2 proximity sensors will be mounted on back layer chambers using special brackets (pinned in the panel 1 alignment sensor reference holes). They will sense the corner frame mounting brackets

6.2 The R and Z sensor calibration.

The physical position of the R and Z-sensors, with respect to their base plates or brackets, can be calibrated to an accuracy of about 100 μm. For the transfer plates, this measurement defines the local Z position of the SLM reference sensor. For the R sensors, this will determine the strip relationship on the top panel of the CSCs. This data plus the readout offset and slope calibration as described above goes into the database for reconstruction.

6.3 Initial Alignment.

The transfer-plate at ME3, the farthest station in the de-scoped scenario, will support the laser that defines the EMU transfer-line. The laser and transfer-sensor can be moved several millimeters (calibrated adjustment) in the Rϕ plane, until the laser beam and transfer-sensor are more or less centered on the 2-D sensors on the MABs. The adjustment technique has not been defined yet, but it will be tuned for transmission across both endcaps. The reference sensors on the MABs define the R and ϕ coordinates (the line extensions). As long as the laser beam falls near the center of those sensors, its actual direction will be accurately known and there will be dynamic range for movement. Other transfer-plates have calibrated adjustments of the transfer-sensor in the Rϕ, and R directions.

During installation, the transfer plates will be pinned and mounted to a bar on an universal extension support on the iron discs. This rigid tube extension support mounts and pins to corner connection plates mounted into machined pockets in the iron. These corner plates and machined pockets are positioned to one or two millimeter accuracy. The ϕ, Z position/rotation will be established by the

support referenced to the endcap iron connecting plates [provided by the Integration group] on the machined areas of the endcap iron rings. The orientation of the transfer-plate will be defined by two angle inclinometers set on precision wedges to compensate the nominal ϕ angle of the transfer line. The two opposite transfer-plates are also coupled by the Z referencing. The use of DCOPS, with their sensitivity to transverse rotations, could simplify the transfer-plate installation.

The other transfer-plates (at ME1 and ME2) will be installed after the end transfer-plates. In an up-scope scenario, the ME3 transfer plates becomes the ME4 system..

6.4 The R and Z sensor installation

The R potentiometer, which measures the R position of the CSC nearest to the transfer-plate, will be mounted and calibrated on the outer SLM plate. A cable extension of the sensor will be hooked to the transfer-plate in situ. The Transfer Z sensors will be attached to the transfer-plate directly, and will monitor the relative end position of the Z transfer tubes. These Z sensor will be measured and calibrated on the transfer-plate in relation to the SLM endpoint sensor position.

6.5 Photogrammetry

Photogrammetry survey can locate the chamber relative positions, in a zero-field open-Endcap situation, to about 250 - 300 micron in the transverse positions **provided** that many overlapping smaller camera fields are bundled. Using the photogrammetry as a cross reference, each CSC layer position monitoring straight line monitor will be checked for relative position accuracy in measurement by operation during the open layer survey. Photogrammetry measurements of the transfer-plates (via pre-calibrated targets), CSC alignment sensors/brackets (via tape spot targets on brackets), and targets on the alignment pins will provide the set of cross-references. This is a useful test of the accuracy of the layer alignment system before the Endcaps are closed and the magnet energized.

The required photogrammetry will be carried out by CERN. After consultation with the CMS Technical Coordinator, last year (1998), the EMU Alignment budget was reduced by the amount estimated for the photogrammetry survey.

7. Error Analysis.

The errors that contribute to the ϕ measurement error of a chamber are due to

1). The CSC SLM laser line
2). The sensor measurement (5 μm, short term)
3). The sensor positioning (25 μm)
4). The plate positioning (50 μm)
5). The strip referencing (75 μm)
6). Temperature deformation (20 μm)

Some of the numbers in parenthesis have been measured (2), others calculated (6) and the rest are best estimates. The estimate for (3) and (4) are different because one measurement will be done in the lab and the other in situ.

The direction of the CSCs laser line is defined by two points, P_1 and P_2, diametrically opposed (about 14

m apart), on the periphery of the Endcap iron (see **Fig 6**). The uncertainties in each of these two points arise from the errors due to:

7). The EMU transfer laser position at the transfer-plate
8). The transfer 2-D sensor (or laser) uncertainty (25 μm)
9). The transfer 2-D sensor (or laser) position (50 μm)

In the EMU transfer-line, the ϕ measurement is also done with respect to a laser line whose direction is defined at two points, M_1 and M_2. These two points are about 13 meters apart, on the MABs at each end of the CMS Barrel. The errors in M_1 and M_2 (see the Error Table that follows) have been estimated to be

$$\Delta M_1 = \Delta M_2 \sim 90\ \mu m$$

A two-point line error.

The perpendicular position uncertainty, ΔY, at a given point in a line defined by two points is given by

$$SQRT\ [(1+K)^2 + K^2],$$

multiplied by the error of one reference points, assuming that the two points have equal errors. K, in that expression is equal to $(L_1 - L)/(L_2 - L_1)$, where L, L_1, and L_2 are respectively, the position of the sensor, and of the two reference points, along the laser line.

Error (7), the transfer laser position error, is given by,

$$\Delta Y_M * \Delta M_1 \sim 95\ \mu m$$

At the EM2,3 stations the P_1 error is the quadratic sum of errors (7), (8), and (9), that is

$$\mathbf{\Delta P_1 \sim 113\ \mu m}$$

Error (1) is then given by $\Delta Y_P * \Delta P_1$. In the case of CSC laser, the reference points are at the extremes of the line, and the error at any given point in between is smaller than at the reference points themselves. In other words $\Delta Y_P < 1$. Thus, error (1) is smaller than ΔP_1.

The Rϕ alignment error is then, after adding all errors (1) through (6), in quadrature,

$$\mathbf{\Delta\ R\phi = 140\ \mu m}$$

7.1 R-dependent corrections on ϕ

In Sections 4.2 and 4.3 We discussed at some length the fact that a relatively small R misalignment (< 1mm) could have a sizable effect in the ϕ determination of a muon track. Here we discuss the effect of the relatively coarse R resolution of the chambers (16 to 51 mm in granularity). It does not affect the ϕ measurement, except, when there is a misalignment in ϕ, that is, when the chamber strips are rotated (around a Z-axis) with respect to the corresponding radial lines. In that case, a ϕ correction must be

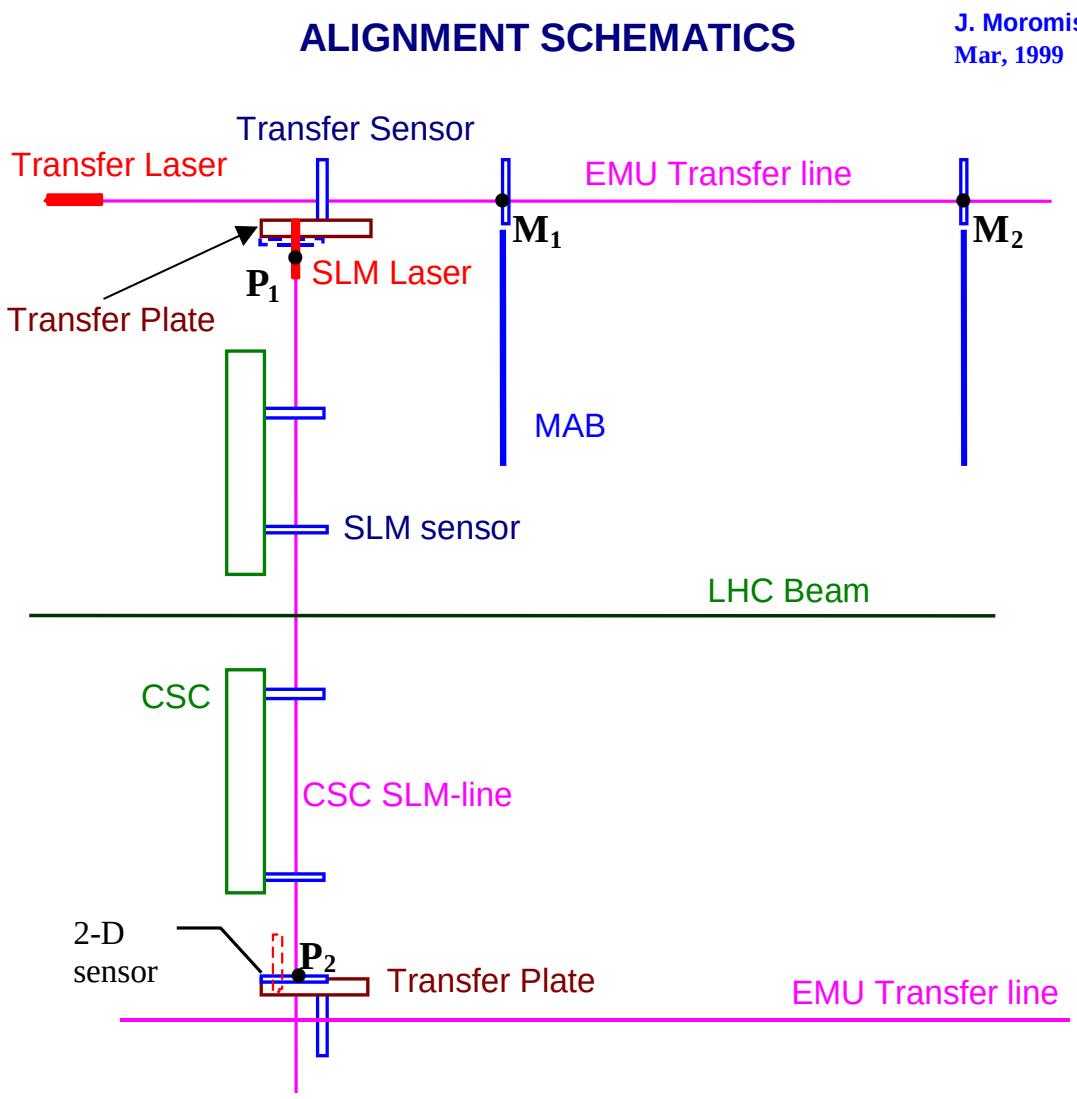

Fig 6. ALIGNMENT SCHEMATICS. Only one transfer laser is shown, at the top-left corner, defining the EMU transfer line. Similarly for the SLM line, only one laser beam, coming from the top is shown. The other laser beams coming from the opposite directions have been omitted for clarity.

applied which depends on R; this raises the question of whether the R resolution of the CSCs is compatible with the ϕ calibration requirement. In other words, given the large uncertainty in the R measurement, can we expect to apply a ϕ correction to each hit within the required accuracy? The answer is yes, provided that the CSCs rotation with respect to a truly radial orientation, can be kept below a few milliradians. The R resolution of the CSCs is below 15 mm (the rms of a 51 mm square distribution), therefore the Rϕ uncertainty in would be 15 μm per milliradian of rotation misalignment in the CSCs. The expected angular misalignment is smaller than one-milliradian, given the error constraints on the machining of the CSC support holes in the iron plates. We conclude that the ϕ correction, even an R dependent one, can be made to the required resolution in Rϕ.

7.2 Rϕ Error for Overlapping CSCs

Only chambers along the SLM laser lines, which we will call chambers 'A', will be directly monitored by the alignment system. The neighboring chambers ('B') in ME2, and ME3, will be aligned through actual particles hits on the overlapping sector of the chambers. Each particle detected with coordinates R, ϕ^a in an A-chamber will have a counterpart hit in the overlapping B-chamber with coordinates R, ϕ^b. We assume that the R coordinate is common to both chambers. If the misalignment is such that $\phi^a - \phi^b$ is R dependent (which means the overlapping strip are not parallel), then an R dependent correction must be applied to the B-chamber. The R resolution of the chambers is, as mentioned above, consistent with the required Rϕ maximum error. Therefore, the Rϕ alignment error of the B-chambers will be comparable to that of the A-chambers. How many hits in the overlapping region will be needed to align the B-chambers? In principle, two hits far apart in R would be sufficient. In practice, many more than that could be needed. Monte Carlo studies will be undertaken to get a more precise answer.

8.1 Summary Table for Expected Alignment Precision.

EXPECTED ALIGNMENT ERROR (in μm)

	Rϕ	**R**	**Z**
ME1/2	78	69	90
ME1/3	90	77	190
ME2/1	128	186	210
ME2/2	139	153	210
ME3/1	135	186	222
ME3/2	147	153	222

9. Requirement on Chamber construction

9.1 Strip referencing accuracy

A look at the Error Estimates shows that the Rϕ errors are dominated by the strip referencing errors, both at the construction stage and afterwards. The external fiducial points should be referenced to the actual strip positions to better than the just specified requirements. This means that the Rϕ location of the strips should be accurate to 75 microns, for the ME1/2 and to 150 microns, for the other stations. This can be ensured by sample panel measurement providing variances are within this bound.

In addition, the strip R-positions must, during the construction process, be determined relative to external fiducial references to better than 860 microns (430 microns for the 20-degree chambers). The corresponding allowable error for the ME1/2,3 chamber is 430 microns. The absolute R-sensors along SLM lines are mounted on the same sensor bracket as the Rϕ, Z optical sensor. So CMM measurements of sample panels for each type of CSC will also provide the absolute R position data on strips relative to alignment holes and pins (see below).

We plan to directly pin our measurement sensors into the top cathode panel of the CSC assemblies. These pin locations will be established on the Axxiom machine at the same time as the alignment pin

hole and slot as through holes within the gap bar area on both the wide and short ends. Clearance holes are made in the frames. Hold-down screws attach to the frame. When the reverse side cathode strip configuration is machined on the Gerber, we propose to include cutter notches (y, x as possible) around the alignment pin hole/slot at a programmed offset to the nearest strip edge (cut). We propose to measure a sample of these panels (inside face) on a large CMM machine (Rockford, IL or the Indiana facility) capable of measuring the whole panel to establish the real strip positions, the relationship of the alignment holes, and the reference cut marks on the panel (both holes-both ends). For the alignment holes, we would measure target inserts. The CMM measurement errors should be well within 25 μm. In particular, we can then establish the relationship of the notches and strips (local to the alignment holes). Subsequent sampling of the local notch-alignment hole target (local microscope or camera system) relationship at each end will provide checking of the pins-strip system relationship. This can be done on every panel 1 if necessary. To check the cutting program for every CSC type, we should do the CMM sample measurement for every CSC type. Given the alignment pin-hole tolerance relationship(<2 mils), we should be able to flip the panel and use the alignment holes/pins to gauge measure SLM alignment sensor pin mounting holes to ~1 mil. So it seems possible to relate the sensor brackets to the internal strip pattern (on panel 1) to a few mils. We propose to establish a "standard calibration fixture for position sensor/bracket assembly measurements (all DOF)" which will provide a sensor position/orientation relative to the two bracket mounting pins/holes to ~ 1 mil. Further we plan that each sensor bracket will include a photogrammetry tape target set (multi spot targets) that has been measured and referenced to the sensor in the calibration bench. The big reference question arises for the sensors that must mount on towers (~30cm tall) on the backlayer ME3/2, ME2/2 chambers (part of the supersymmetry deal!). At present we continue to locate these with the same two pins as for "direct mount sensor brackets"; and depend on the extrusion straightness for perpendicularity. We will need to do some tests and sample measurements, so the alignment sensor-panel 1 relationship can be known to a few thousandths of inch. Because of tolerances on the alignment pins, panel holes, hole edges and hole distortion under load (rotation in bare CSC assembly), it is possible to have a random transverse shift of panel positions and pins that are not perpendicular to the CSC stackup. While the "scatter" of panel positions can be corrected for in local track fits, the issue of a systematic shift across the layers seems difficult to unfold. Some ideas about theodolite measurement of targets on the ends of temporary long alignment pins (after frame assembly and bolt torquing) have been discussed. We have also requested tighter hole tolerances through all CSC panel at the 1D CSC mount to control the phi position and panel stackup more accurately.

10. System Architecture

10.1 Power, Readout, and Control.

Every sensor will have to be powered and read out. Light sources and position adjustment devices will in addition require control inputs. These will be provided for through programmable boxes, based on simple CPUs or DSPs, scattered throughout the Endcap region..

For EM2 and EM3 the alignment sensors are more or less clustered around 6 points, or nodes, on the periphery of the common endcap iron disk. Since the Endcap disk will move independently of the others, the cables connecting the alignment elements must be attached to a single Endcap disk. Power lines and signal cables will be strung towards the sensors and other devices along R segments (constant phi and Z), containing the EMU Transfer plates and the corresponding SLM arrays, from

each of the node boxes on the iron disk. The R and Z sensors are located near the SLM lines and will also be connected to the same node. The maximum distance device-node will be around 10m. Each of the 12 node boxes (6 per Endcap) will in turn be controlled and powered through one, or possibly more than one, computer sitting at a main-node. The main-node will be located in an accessible place near CMS, and will be networked with each of the nodes it controls and eventually with the global CMS Slow Readout system.

The node boxes will, possibly, be connected through Ethernet lines to the main-node computer(s). The connection node-sensor will be DC level, i.e. slow analog signal, except where a serial line is needed (for DCOPS, for instance).

The present design of the DCOPS boards includes some of the desired capabilities, and it could be modified to work as one of the nodes mentioned above. A similar arrangement will be explored for the Almy sensors.

The sensors in the ME1 Variation, and those located on the MABs, can also be connected in a similar manner, thus increasing the number of nodes.

11. Redundancy and Device Failure Analysis

There are two types of failures we will be concerned with: device breakdown and bad data. Device breakdown occurs when a device (sensor or laser source) can not be readout or controlled. 'Bad data' is when the sensor is out of calibration (have been knock out of position, for instance). A robust design should allow the system to function even when some of the devices breakdown or give bad data. If a device can not be read out reliably, the bit of information it does supply is no longer useful. We can analyze the effect of such failure for each of the five types of sensor arrangements discussed in Sec 3.1.

The EMU Transfer lines is made up of the following elements:

a) Laser sources: there will be two of them and only one is required to define the transfer line.
b) Reference sensors (on the MABs): there are two of them per Transfer line. Both are necessary to define the Transfer line. No redundancy here, but as stated below there are twice as many Transfer lines as required to position the endcaps.
c) The station sensors: Each one will determine the location the Transfer plate on which an SLM laser source mounted. If the sensor fails then the information from that particular SLM is unreliable.

However, only three Transfer lines (out of the six that will be used), together with equal number of Z-sensors, are really necessary to locate each of the iron plates of the endcaps. Thus the system has a high degree of redundancy as far as the EMU Transfer lines are concerned.

The Z Tubes arrays, as mentioned above, have as much redundancy as the Transfer lines, namely more than 50% of them must fail before affecting the accuracy of the alignment data (assuming, of course, that the iron distortion is mostly Z dependent)

The SLM arrays may be subjected to a very specific failure mode, namely the one caused by a possibly larger than expected Z distortion of the iron disks, due to the solenoidal magnetic field. If the Z distortion is larger than about 25 mm then the SLM laser beam will move beyond the sensitive area of the 2-

D sensors thus making the ϕ and Z measurements unavailable. Sensor with larger Z range could be used wherever the Z distortions go beyond the reach of our normal 2-D sensors, but the optical path aperture could then become the limiting factor. In addition there are some risks to the optical paths as defined, in particular when going through the core of the Endcap support pipe (another experiment, TOTEM, will be installing devices and cables there).

However, the SLM arrays can fail 100% and one could still locate the phi coordinate of the CSCs, from the position of the iron plates (given by the Transfer lines and Z tubes), on which the chambers are mounted, and from the photogrammetry survey data (provided the survey resolution is adequate). The overlap strips, between neighboring chambers, can confirm (through common tracks) the relative location of the chambers, both in phi and R, and allow alignment correction on those coordinates. Only the Z coordinate measurement, at low R, will be badly affected, thus the deployment of additional Z measurement devices will be advisable.

The R-sensors, in each of the stations, are redundant with the survey data. Namely, photogrammetry survey will give us the position of each CSC with respect to the iron plate that supports it. Thus, knowing the position and orientation, of the iron plates we can deduce the R position of the CSC in real space, real time. And, as mentioned above, muon tracks through the overlapping strips should pinpoint any miss-aligned chamber, in R, and determine the actual correction parameters.

In conclusion, only the Z measurement lacks adequate redundancy. This can be fixed by the addition of 6 (or 12) sensors per station. That means a total of 36 (or 72) new sensors in the EMU Alignment system. On the positive side, the Z location of the chambers is not so critical: resolutions of around 1mm will suffice.

The ME1 Variation is more dependent on the Link Alignment system, not only in the latter's referencing to the Tracker position but on the viability of its technical solutions as well. This is clearly an area that needs further analysis and close cooperation with the Link Alignment group.

12. Alignment Simulation

There is at present no software to simulate the performance of the EMU Alignment System. Simulgeo, the alignment simulation program developed by Laurant Brunel at Cern, has been designed around digital cameras and point light sources, such as those used in the Barrel Muon Alignment. Pedro Arce, with the Link Alignment group, has now a new version (Simulgeo++) that can accommodate optical arrangements using laser beams and transparent 2-D sensors. We should be able to start simulation studies this summer.

13. The Alignment Database.

In a block diagram of CMS the Alignment System could be represented by a simple box with input and output lines. The output lines would contain, primarily, the values of the parameters needed to locate the tracking chambers. And the input will consist of sensor positions, readings, correction and calibration factors; photogrammetry data, chamber geometrical parameters, etc.
The alignment database should make these, and other relevant information, available to the CMS community in a timely and accessible fashion.

Although the overall alignment group has not yet addressed this important issue in a coordinated way, it should be useful to present some of our very preliminary ideas here. At least two separate, but related, database files, or sets, could be maintained by the Alignment Group. One set could contain all the input information, for instance the sensor readings, while the other could have the output information, for instance the latest position of each of the chambers in the system.

We are working on the outline of such database. Naming conventions, for instance, have been adapted to the CMS Integration standards. It includes definitions, sensor labels, sensor identification, references, and locations in the CSC local coordinate system (survey data subject to rigid body ensemble translations/rotations), offsets, calibration constants of sensors, status, etc. This could become the information base for a geometry reconstruction program. The table that follows shows a tentative labeling scheme for the alignment elements and some of their basic parameters.

14. Integration Issues.

Physical locations for the different alignment components, as well as optical pathways for the SLM sensors, have been determined with the help of the Endcap Integration Group. We are working on details with this group and the CERN Integration group to solve integration and cross requirement issues. We will also work in detail with the CSC production group to provide necessary information, achieve appropriate reference measurements, and assembly control and tolerances.

The preliminary design of the alignment system had the optical pathways contained on R-Z half-planes, that divided the CMS detector into 6 equal longitudinal sectors. Unfortunately, that simple 60-degree symmetry was incompatible with the Barrel Muon geometry, which has mirror symmetry about a vertical plane parallel to Z. That forced the optical path for the EMU transfer slightly off the 60-degree symmetry. These current pathways have been certified through the Barrel system. The pathways of the Z transferring have been established as well.

Because the CSC arrangement has a 60-degree symmetry, the SLM lines were selected to cross the CSCs at the same relative position within mirror symmetry. This meant that only two sets of reference/attachment holes have to be made on the CSCs. The endcap transfer optical paths are forced in position by the junctions of MB4 barrel chambers (only approximate 60-degree symmetry). This dictates a set of four (and mirror versions) different transfer plates. As it turns out, at position 5 (255 degree) the iron disc support structure dictates another variant of the transfer plate. At this time, the positions and parameters of all transfer plates and Z transfer tubes have been finalized in the integrated layout.

Locations of slots of appropriate dimensions have been specified in the contract for the endcap steel, to accommodate the SLM optical paths through the yoke spacer. We are working on a specification of these apertures to the CERN Integration group through the TOTEM chamber system (Z+, Z-).

15. The Endcap Alignment Group

The alignment group consists of the following physicists: J. Moromisato (co-leader), E.von Goeler, and S. Reucroft, from Northeastern University; and D. Eartly (co-leader), and K. Maeshima, from Fermilab. The following table lists the manpower available at each of the two institutions for the EMU alignment effort.

EMU Alignment Group

Name	Institution	% of Rsch Time	Interest
J. Moromisato	Northeastern U.	100	Instrumentation, MC
E. Von Goeler	Northeastern U.	80	Hardware, MC
S. Reucroft	Northeastern U.	30	P.I.
D. Eartly	Fermilab	100	Hardware, Instrumentation
K. Maeshima	Fermilab	50	MC

16. Responsibilities for the EMU Alignment System

The responsibilities for the different tasks associated with the EMU Alignment Project are distributed according to the table that follows. Each of the tasks is assigned to one of the two Co-leaders of the project, to be carried out, preferentially but not necessarily, at the specified institution. While the responsibilities are defined according to tasks, there is significant interleaving of efforts and cooperative decisions.

WBS No.	Description	Institution
1.7	***Alignment***	
1.7.1	Global alignment	
1.7.1.1	barrel z connection	Eartly
1.7.1.1.1	design barrel z connection	Fermilab
1.7.1.1.2	procure barrel parts	Fermilab
1.7.1.1.3	Calibrate & test	Fermilab
1.7.1.1.4	install barrel z conn.	Fermilab
1.7.1.2	**endcap z connection**	**Eartly**
1.7.1.2.1	design endcap z connection	Fermilab
1.7.1.2.2	procure parts (3)	Fermilab
1.7.1.2.3	Calibrate & test 1	Fermilab
1.7.1.2.4	procure endcap z parts (9)	Fermilab
1.7.1.2.5	Calibrate & test 2	Fermilab
1.7.1.2.6	procure endcap z parts (9)	Fermilab
1.7.1.2.7	Calibrate & test 3	Fermilab
1.7.1.2.8	procure endcap z parts (15)	Fermilab
1.7.1.2.9	Calibrate & test 4	Fermilab
1.7.1.2.10	install endcap z	Fermilab
1.7.1.2.11	procure spare Z4D sensors (3)	Fermilab
1.7.1.3	**transfer system**	**Moromisato**
1.7.1.3.1	design transfer plate	Northeastern
1.7.1.3.2	procure prototype transfer plate	Northeastern
1.7.1.3.3	procure z+ transfer assemblies	Northeastern
1.7.1.3.4	procure transfer sensors (12)	Northeastern
1.7.1.3.5	test sensors 1	Northeastern
1.7.1.3.6	procure transfer sensors (12)	Northeastern
1.7.1.3.7	test transfer sensors 2	Northeastern
1.7.1.3.8	procure z- transfer assemblies	Northeastern
1.7.1.3.9	procure transfer sensors (16)	Northeastern
1.7.1.3.10	test sensors 3 & install	Northeastern
1.7.1.4	**rasnik system**	**Moromisato**
1.7.1.4.1	design rasnik plate	Northeastern
1.7.1.4.2	procure prototype rasnik plate	Northeastern
1.7.1.4.3	procure +z rasnik plates (6)	Northeastern
1.7.1.4.4	install +z sensors	Northeastern

1.7.1.4.5	procure -z rasnik plates (6)	Northeastern
1.7.1.4.6	install –z sensors	Northeastern
1.7.2	**Local alignment**	**Moromisato**
1.7.2.1	Straight line monitor (SLM)	Moromisato
1.7.2.1.1	**ME1 SLMs**	**Moromisato**
1.7.2.1.1.1	design SLMs	Northeastern
1.7.2.1.1.2	procure SLM sensors (18)	Northeastern
1.7.2.1.1.3	procure SLM sensors (60)	Northeastern
1.7.2.1.1.4	test & calib. SLMs	Northeastern
1.7.2.1.1.5	install SLMs	Northeastern
1.7.2.1.2	**ME2 & ME3 SLMs**	**Moromisato**
1.7.2.1.2.1	Design SLMs	Northeastern
1.7.2.1.2.2	procure prototype ALMY sensors (2)	Northeastern
1.7.2.1.2.3	procure prototype digital sensors (6)	Northeastern
1.7.2.1.2.4	develop COPS sensor system	Northeastern
1.7.2.1.2.5	procure serial interface	Northeastern
1.7.2.1.2.6	procure SLM sensors (120)	Northeastern
1.7.2.1.2.7	test & calib. slms	Northeastern
1.7.2.1.2.8	install SLMs	Northeastern
1.7.2.2	**Radial sensors**	**Eartly**
1.7.2.2.1	design and prototype sensors	Fermilab
1.7.2.2.2	procure prototype radial sensors (6)	Fermilab
1.7.2.2.3	procure sensors (72)	Fermilab
1.7.2.2.4	test & calib. sensors	Fermilab
1.7.2.2.5	install sensors	Fermilab
1.7.2.3	**Proximity sensors**	**Eartly**
1.7.2.3.1	**ME1/3 Prox. Sensors**	**Eartly**
1.7.2.3.1.1	begin proximity design	Fermilab
1.7.2.3.1.2	procure prototype proximity sensors (12)	Fermilab
1.7.2.3.1.3	finish proximity design	Fermilab
1.7.2.3.1.4	procure sensors (132)	Fermilab
1.7.2.3.1.5	test & calib. sensors	Fermilab
1.7.2.3.1.6	install sensors	Fermilab
1.7.2.3.2	**ME1/2 Prox. Sensors**	**Eartly**
1.7.2.3.2.1	design system	Fermilab
1.7.2.3.2.2	procure sensors (144)	Fermilab
1.7.2.3.2.3	test & calib. sensors	Fermilab
1.7.2.3.2.4	install sensors	Fermilab
1.7.2.3.2.5	procure spare proximity sensors (15)	Fermilab
1.7.2.4	**Laser system for SLMs**	**Moromisato**
1.7.2.4.1	design laser system	Northeastern
1.7.2.4.2	procure laser diodes (39)	Northeastern
1.7.2.4.3	test & mount diodes	Northeastern
1.7.2.4.4	install laser diodes	Northeastern
1.7.2.5	**Temperature sensors**	**Eartly**
1.7.2.5.1	design temperature sensors	Fermilab
1.7.2.5.2	procure temp. sensors (500)	Fermilab
1.7.2.5.3	install temp. sensors	Fermilab
1.7.3	**Alignment Readout System**	**Moromisato**
1.7.3.1	design system	Northeastern
1.7.3.2	procure parts	Northeastern
1.7.3.3	procure LV	Northeastern
1.7.3.4	procure serial cabling & interfaces	Northeastern
1.7.3.5	test & calib. system	Northeastern
1.7.3.6	install & debug at CERN	Northeastern
1.7.4	**Calibration & Testing**	**Moromisato**
1.7.4.1	design calibration system	Northeastern

1.7.4.2	design testing system	Northeastern
1.7.4.3	procure parts for testing	Northeastern
1.7.4.4	set up testing system	Northeastern
1.7.4.5	Integrated testing of prototypes	Northeastern
1.7.5	**System Installation**	**Moromisato**
1.7.5.1	Setup & testing at CERN	Northeastern

17. Engineering Work Plan for 1999

The system requires a major engineering effort on the system elements in 1999 to meet CMS milestones including prototypes for the ISR system proof of principle test and element designs and drawings which satisfy the CMS Integration requirements prior to the system Engineering Design Review at the end of 1999.

To meet these needs, we have initiated a contract design effort with the Physical Sciences Laboratory Engineering-Integration group (University of Wisconsin) and have invited a guest engineer (from PNPI, Russia) to Fermilab. We hope to continue collaboration with PNPI in the future to provide continuity in the project.

DCOPS detector engineering development has also been in progress at Fermilab for some time. We plan to have this increase in the event of a positive DCOPS detector decision in June 1999. In addition, some additional electrical engineering work will be required on the corresponding serial readout ADC system for other sensors (Z, R, T) as well as T sensor, Z sensor gating electronics boards. This is within the capability of the electrical engineering service group in PD at Fermilab given corresponding support from project funds (1.7.3.1 Readout system design). Design approval and revisions to meet system requirements will be a joint decision by D. Eartly, F. Feyzi, J. Moromisato, and R. Loveless.

Design Projects and the Nominal Design Group:

WBS No.	Task	Design Group	Comments
1.7.1.3.1	Transfer-plate designs	Led by PSL Integ/Eng	FNAL cooperates in detail
1.7.1.4.1	MAB sensor plate	FNAL design	in cooperation with PSL/CERN Integration
1.7.2.1.1.1	ME1 SLM design	FNAL design	in cooperation with PSL/CERN Integration
1.7.2.1.2.1	ME2/ME3 SLM design	Led by PSL	FNAL does brackets, CSC panel mods.
1.7.2.2.1	Design/proto R sensors	FNAL design	in cooperation with PSL/CERN Integration
1.7.2.3.1	Start Proximity design	FNAL design	in cooperation with PSL/CERN Integration
1.7.2.5.1	Temp Sensor/Readout	FNAL design	in cooperation with Northeastern

Northeastern and Fermilab will begin a joint effort in preparing all necessary data, specifications, test results, design analyses, element drawings, safety analyses, reliability analyses, etc for the CERN Engineering Design Review.

18. Schedule

TASK	START	FINISH
2-D Sensors Decision	Jun.99	
Procure/test	Jun.00	May.02
Laser sources	Jun.00	May.02
Transfer-plates Prototypes	Sep.99	Mar.00
Procure/test	Jun.00	Mar.02

Transfer Ref sensor hardware	Jun.01	May.02
CSC SLMs	Jun.01	Mar.03
Integrated test	Sep.99	
R-sensors	Jun.00	Sep.01
Z-sensor	Mar.00	Jun.01
Temperature Sensors	Jun.00	May.02
Readout system	Jun.00	Jun.03
Calibration/testing	Mar.01	Mar.04
Installation	Sep.03	Sep.04

19. Funding Profile

Year	Amount (in K$)
1998	30
1999	62
2000	150
2001	120
2002	100
2003	100
2004	100
Total	**662**

20. Need for Change request.

If it is concluded that the R position of the CSCs as measured by photogrammetry is NOT adequate or stable (field on vs field off), then the EMU Alignment must be able to measure the absolute R displacement of ***every single*** CSC to the required accuracy. This fact has not been considered in the current design of the alignment system, therefore suitable changes must be made. They are, fortunately, incremental rather than conceptual in nature. As described earlier, the EMU Alignment has a completely modular design, which means that performance characteristics of different groups of sensors are quite independent of each other. The required change to the alignment design will consist of the addition of one R-sensor per chamber (except for those that are already provided with it). 360 – 72 = 288 ==> ~$60K, excluding the ME1/1s. Other related costs, such as calibration, cabling, and installation, have to be added as well. An answer to this question can only come after a detailed target procedure proposal to the CERN geodesy group plus a careful look at the iron distortion model.

We do believe that the information in photogrammetry will be greatly improved if we outfit all CSCs with a photo target cluster at all possible alignment sensor locations. We will look into the design of two simple brackets that can be easily calibrated and which uses low cost photo tape target strips. Our goal is to provide a calibrated target set for each CSC at a cost of $100-$150 per CSC ($28.8K-$43.2K).

An earlier Change Request made by the Northeastern group asked for additional funds for technical support. That request (CR020) for $152K was deferred pending a review of the EMU Alignment Project. The responsibilities assigned to Northeastern (Section 13) include many labor intense activities such as testing, calibration, assembly and installation of the different components of the system. The funds for technical support, included in the present Alignment Budget, are not sufficient to hire a full time technician, which has already led to serious delays in several tasks, hence the change request. We plan to resubmit CR020 as soon as the review is completed.

21. The Choice of Sensors

We are required to make a documented decision to CERN LHCC before the end of June 1999 on a baseline change of optical position detectors. The decision on the choice of ALMY or DCOPS will be based on the consideration related to requirements, redundancy, technical features, status, test results, costs, availability, reliability, long term stability, risks, radiation tolerance, maintenance, and failure modes. A list of the relevant issues for each of the two type of sensors follow.

The ALMY issues are:

- ALMY II status,
- Detector-electronics configuration
- Results of new ALMY tests
- Cost and availability
- Optical transmission and uniformity,
- Aging and reliability,
- Radiation tolerance of electronics,
- Production schedules,
- Signal levels for low output laser,
- Fiducialization and calibration,
- Dimension compatibility and or detector-electronics splitting,
- Noise, power, and grounding consistent with CSC requirements,
- Failure modes must be demonstrated to result in single sensor loss,
- Compatibility to CMS readout/data transfer requirements with the global muon alignment.

The DCOPS issues are:

- Successful test of multi DCOPS readout,
- Adequate radiation tolerance of CCDs and electronics (prom, DSP),
- Measurement of tolerance to dark current increases (fit and thresholds),
- Stable absorber/diffuser (long term),
- Laser source results and temporal line and shape stability,
- Calibration procedures on CCD positions
- Prototype of bi-directional sensor for redundant measurement and non critical detectors (connection detectors for opposing lasers),
- Prove serial passthrough in failure (downstream detectors still readout),
- Adapt to supply voltage,
- Make regulators that work in medium and high magnetic field, noise, power, and grounding
- consistent with CSC requirements, and
- Compatibility to CMS readout/data transfer requirements with the global muon alignment.

We believe that the decision will have to be delayed until the cost/availability of AMLY II and all of the technical issues of both detectors can be resolved.

Given the detector decision, we will work with the CSC chamber and electronics groups as well as the global alignment group and CMS Slow control group on readout protocol and grounding issues.

22. The ISR Test

As a demonstration of the performance of the described position monitoring system given anticipated input from the Link and Barrel alignment system, we will set up a hardware prototype of one branch of the Endcap transfer line system with connection to a corresponding SLM in ME2. This will involve a complete prototype of the transfer-line with MAB definition sensors, transfer-plates, Z transfer tubes, transfer-line sensors, SLM sources, sensors, and a prototype readout system. Part of the test will be to establish the global readout and analysis. This test will begin in the fall of 1999 with preliminary results available for the Engineering Design Review. Some design and preparation is underway. It will be a joint effort of Northeastern and Fermilab.

References

[1] CMS Muon System Technical Design Report, Chapter 7; Muon Alignment Group, CERN/LHCC 97-32.

[2] Transparent Silicon Strip Sensors for the Optical Alignment of Particle Detector Systems, W. Blum, H. Kroha, P. Widmann, Max Planck Institute for Physics/MPI-PhE/95-13

[3] A Novel Laser Alignment System for Tracking Detectors using Transparent Silicon Strip Sensors, W. Blum, H. Kroha, P. Widmann, Max Planck Institute for Physics/MPI-PhE/95-05

[4] International Alignment Workshop at MPI, Munich, April 98; see http://pcatlas4.mppmu.mpg.de/mdt/library/alignment_workshop.htm

[5] COPS Position Monitoring System for the CMS Endcap Muon System; D. P. Eartly, T. F. Droege, E. Hahn, R. H. Lee, D. O. Prokofiev, J. Moromisato, E. von Goeler, CMS Note 1996/021.

[6] A Two Dimensional Digital CCD Optical Position Sensor for Relative Alignment Monitoring; D. P. Eartly, S. Hansen, T. F. Droege, D. O. Prokofiev, J. Moromisato, E. von Goeler, Fifth Intl Workshop on Accelerator Alignment, Oct 97, see http://eartly.fnal.gov/empms/ or http://www.aps.anl.gov/conferences/iwaa97/iwaa97.html

[7] Study of position resolution with COPS; J. Moromisato, E. von Goler, S. Reucroft, D. Eartly, T. Droege, D. Prokofiev, Nucl. Inst. And Meth. A426 (1999) 375.

[8] CMS Endcap Muon System Evaluation of MPI Transparent Amorphous Silicon - X, Y Strip Readout Optical Beam Position Sensors; D.P. Eartly, R. H. Lee, A. Bujak, D. O. Prokofiev, CMS IN 1997/005.

[9] CMS Endcap Muon System Tests of MPI Transparent Amorphous Silicon - X, Y Strip Readout Optical Beam Position Sensors in two way split Laser Diode Module Beams; D.P. Eartly, R. H. Lee, CMS IN 1997/020.

[10] CMS Endcap Muon System Long Term Resolution Tests of MPI Transparent Amorphous Silicon Optical Beam Position Sensors in a Multi Sensor Straight Line Monitor; D. P. Eartly, R. H. Lee, CMS Note 1998/004.

[11] CMS Endcap Muon System Tests of a Link Straight Line Monitor R, Rϕ, Z using MPI Transparent Amorphous Silicon Optical Beam Position Sensors, Laser/LED Z distance sensors, and R wire displacement potentiometers; D. P. Eartly, R. H. Lee, (CMS Note 1998/076); also see http://tycho.physics.purdue.edu/~leer

[12] CMS Endcap Muon System Tests of a Link Straight Line Monitor R, Rϕ, Z using MPI Transparent Amorphous Silicon Optical Beam Position Sensors, Laser/LED Z distance sensors, and R wire displacement potentiometers; D. P. Eartly, R. H. Lee, (CMS Note 1998/076)